

New Mixed-Metal Sulfido Metal Carbonyl Complexes by Insertion of Metal Carbonyl Groups into the S–S Bond of CpMoMn(CO)₅(μ-S₂)

Richard D. Adams* and Shaobin Miao

Department of Chemistry and Biochemistry, University of South Carolina,
Columbia, South Carolina 29208

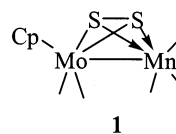
Received February 28, 2003

The disulfido compound CpMoMn(CO)₅(μ-S₂) (**1**) reacted with CpCo(CO)₂ to yield two products, Cp₂MoMnCo(CO)₅(μ₃-S)₂ (**2**) and Cp₂MoMn(CO)₃OC(μ₃-S)₂ (**3**), by insertion of a CpCo group into the S–S bond of **1**. Compound **2** was found to consist of an open MoMnCo cluster with one Mo–Mn bond (2.849(2) Å, one Mn–Co bond (2.605(3) Å, and two triply bridging sulfido ligands. Compound **3** consists of a closed triangular CoMnMo cluster with triply bridging sulfido ligands on each side of the CoMnMo plane. Compound **3** was obtained from **2** by treatment with Me₃NO. Reaction of **1** with Fe₂(CO)₉ yielded the complex CpMoMnFe(CO)₈(μ₃-S)₂ (**4**). Reaction of **1** with Ru₃(CO)₁₂ yielded the ruthenium homologue of **4**, CpMoMnRu(CO)₈(μ₃-S)₂ (**5**), and a minor product, CpMoRu₃(CO)₉(μ₃-S)₂(μ-H) (**6**), that contains no manganese. Compounds **4** and **5** are structurally similar to **2** but contain an M(CO)₃ group in place of the CpCo group. Compound **6** contains a butterfly cluster of four metal atoms with two triply bridging sulfido ligands and one bridging hydride ligand.

Introduction

The disulfido ligand is known to exhibit a variety of bridging coordination geometries,¹ and polynuclear metal complexes containing the disulfido ligand exhibit a range of different structural types.² Metal-containing groups can be inserted into the sulfur–sulfur bond of disulfido ligands leading to mixed-metal clusters containing two sulfido ligands.³ Similarly, small unsaturated organic molecules can be inserted into the sulfur–sulfur bond to yield complexes containing dithiolato ligands.⁴ The simple disulfide of iron carbonyl, Fe₂(CO)₆(μ-S₂), was first reported by Hieber in 1958⁵ and has been extensively investigated over the years.^{2b,2c,3,6,7} Recently, we have reported the new disulfido complexes

Mn₂(CO)₇(μ-S₂)⁸ and CpMoMn(CO)₅(μ-S₂) (**1**).⁹ Compound **1** is structurally similar to Fe₂(CO)₆(μ-S₂), but it contains a Cp ligand on the molybdenum atom in place of one of the terminal carbonyl ligands.



Reactions of Fe₂(CO)₆(μ-S₂) and Mn₂(CO)₇(μ-S₂) with metal complexes generally proceed by insertion of a metal-containing group into the sulfur–sulfur bond (e.g. eqs 1 and 2).^{7,8b,8c}

Mixed-metal sulfido clusters have attracted attention in the past decade,¹⁰ because of possible bimetallic synergistic effects¹¹ in certain types of heterogeneous

* To whom correspondence should be addressed. E-mail: Adams@mail.chem.sc.edu.

(1) (a) Mueller, A.; Jaegermann, W.; Enemark, J. *Coord. Chem. Rev.* **1981**, *46*, 245. (b) Matsumoto, K.; Koyama, T.; Furuhashi, T. *ACS Symp. Ser.* **1996**, No. 653, 251.

(2) (a) Wachter, J. *Angew. Chem., Int. Ed. Engl.* **1989**, *28*, 1613. (b) King, R. B.; Bitterwolf, T. E. *Coord. Chem. Rev.* **2000**, *206–207*, 563. (c) Whitmire, K. H. *Iron Compounds without Hydrocarbon Ligands*. In *Comprehensive Organometallic Chemistry II*; Wilkinson, G., Stone, F. G. A., Abel, E., Eds.; Pergamon Press: New York, 1995; Vol. 7, Chapter 1, Section 1.11.2.2, p 62, and references therein.

(3) (a) Seyferth, D.; Henderson, R. S.; Song, L.-C. *Organometallics* **1982**, *1*, 125. (b) Don, M. J.; Richmond, M. G. *Inorg. Chim. Acta* **1993**, *210*, 129. (c) Cowie, M.; Dekock, R. L.; Wagenmaker, T. R.; Seyferth, D.; Henderson, R. S.; Gallagher, M. K. *Organometallics* **1989**, *8*, 119. (d) Day, V. W.; Lesch, D. A.; Rauchfuss, T. B. *J. Am. Chem. Soc.* **1982**, *104*, 1290. (e) Curtis, M. D.; Williams, P. D.; Butler, W. M. *Inorg. Chem.* **1988**, *27*, 2853.

(4) (a) Koval, C. R.; Lopez, L. L.; Kaul, L. L.; Renshaw, S.; Green, K.; Rakowski DuBois, M. *Organometallics* **1995**, *14*, 3440. (b) Birnbaum, J.; Rakowski DuBois, M. *Organometallics* **1994**, *13*, 1014. (c) Lopez, L. L.; Bernatis, P.; Birnbaum, J.; Haltiwanger, R. C.; Rakowski DuBois, M. *Organometallics* **1992**, *11*, 2424. (d) Rakowski DuBois, M., In *Catalysis by Di- and Polynuclear Metal Cluster Complexes*; Adams, R. D., Cotton, F. A., Eds.; Wiley-VCH: New York, 1998; Chapter 4, p 127.

(5) Hieber, W.; Gruber, J. Z. *Anorg. Allg. Chem.* **1958**, *296*, 91.

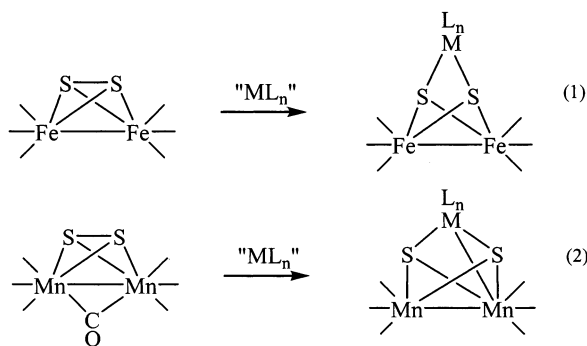
(6) (a) Song, L.-C.; Lu, G.-L.; Hu, Q.-M.; Fan, H.-T.; Chen, Y.; Sun, J. *Organometallics* **1999**, *18*, 3258. (b) Song, L.-C.; Kidiata, M.; Wang, J.-T.; Wang, R.-J.; Wang, H.-G. *J. Organomet. Chem.* **1990**, *391*, 387. (c) Bose, K. S.; Sinn, E.; Averill, B. A. *Organometallics* **1984**, *3*, 1126.

(7) (a) Adams, R. D.; Huang, M. S.; Wu, W. *J. Cluster Sci.* **1997**, *8*, 115. (b) Don, M. J.; Yang, K. Y.; Bott, S. G.; Richmond, M. G. *J. Coord. Chem.* **1996**, *40*, 273. (c) Mathur, P.; Chakarabarty, D.; Mavnkai, I. J. *J. Cluster Sci.* **1993**, *4*, 351. (d) Pasynskii, A. A.; Kolobkov, B. I.; Nefedov, S. E.; Eremenko, I. L.; Koltun, E. S.; Yanovsky, A. I.; Struchkov, Yu. T. *J. Organomet. Chem.* **1993**, *454*, 229. (e) Pasynskii, A. A.; Kolobkov, B. I.; Eremenko, I. L.; Nefedov, S. E.; Katser, S. B.; Porai-Koshits, M. A. *Zh. Neorg. Khim.* **1992**, *37*, 563.

(8) (a) Adams, R. D.; Kwon, O. S.; Smith, M. D. *Inorg. Chem.* **2001**, *40*, 5322. (b) Adams, R. D.; Kwon, O. S.; Smith, M. D. *Organometallics* **2002**, *21*, 1960. (c) Adams, R. D.; Kwon, O. S.; Smith, M. D. *Inorg. Chem.* **2002**, *41*, 1658.

(9) Adams, R. D.; Captain, B.; Kwon, O. S.; Miao, S. *Inorg. Chem.*, in press.

(10) (a) Kabashima, S.; Kuwata, S.; Hidai, M. *J. Am. Chem. Soc.* **1999**, *121*, 1, 7837. (b) Casado, M. A.; Ciriano, M. A.; Edwards, A. J.; Lahoz, F. J.; Perez-Torrente, J. J.; Oro, L. A. *Organometallics* **1998**, *17*, 3414. (c) Ruffing, C. J.; Rauchfuss, T. B. *Organometallics* **1985**, *4*, 524. (d) Hobert Pawlicki, S. H.; Noll, B. C.; Rakowski DuBois, M. J. *Coord. Chem.* **2003**, *56*, 41.



metal sulfide catalysts. Adduct formation of hydrosulfido complexes with heterometal complexes is a practical route to mixed-metal hydrosulfido-bridged complexes.^{10c,12}

We have recently reported that **1** and its Cp* analogue react with a variety of unsaturated organic molecules by insertion into the sulfur–sulfur bond.⁹ We have now investigated reactions of **1** with a few selected metal carbonyl complexes and have found a similar pattern of metal insertions into the sulfur–sulfur bond. These results are reported here.

Results

Two products, Cp₂MoMnCo(CO)₅(μ₃-S)₂ (**2**; 40% yield) and Cp₂MoMn(CO)₃OC(μ₃-S)₂ (**3**; 21% yield), were obtained from the reaction of CpMoMn(CO)₅(μ-S₂) (**1**) with CpCo(CO)₂ at room temperature. Both products were characterized by IR, ¹H NMR, and single-crystal X-ray diffraction analyses. ORTEP diagrams of **2** and **3** are shown in Figures 1 and 2, respectively. Selected bond distances and angles are listed in Tables 1 and 2. In the solid state compound **2** contains a symmetry plane that passes through the three metal atoms. The three metal atoms are arranged in an open triangular cluster; that is, there are only two metal–metal bonds, Mn(1)–Co(1) = 2.6006(17) Å and Mn(1)–Mo(1) = 2.8454(14) Å. The Mo–Co distance is very long, 3.457(1) Å, and is clearly a nonbonding distance. There are two symmetry-related triply bridging sulfido ligands and five linear terminal carbonyl ligands: three on Mn and two on the Mo atom. The cobalt atom and molybdenum atom each contain one η⁵-cyclopentadienyl ring.

Compound **3** also contains three metal atoms: manganese, cobalt, and molybdenum, but these are arranged in a closed triangular group; that is, there are three metal–metal bonds: Mn(1)–Co(1) = 2.5536(6) Å, Mn(1)–Mo(1) = 3.1412(6) Å, and Co(1)–Mo(1) = 2.6784(5) Å. The Mo–Co distance in **3** is very short and clearly indicative of a bonding interaction. The Mo–Mn distance is significantly longer than that in **2** and also in **1**, Mo–Mn = 2.8421(10) Å,⁹ but with the existence of a Mo–Mn single bond, the three metal atoms can all achieve the 18-electron configuration; therefore, we believe that there is probably a Mo–Mn bond in this compound. There is an oxo ligand on the molybdenum atom. The Mo–O bond, 1.706(2) Å, is believed to be a double bond and is similar in length to those in related

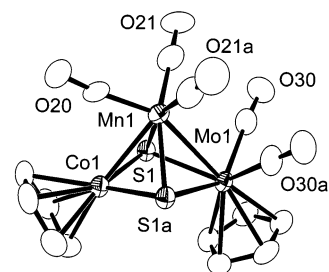


Figure 1. ORTEP diagram of the molecular structure of Cp₂MoMnCo(CO)₅(μ₃-S)₂ (**2**) showing 40% probability thermal ellipsoids.

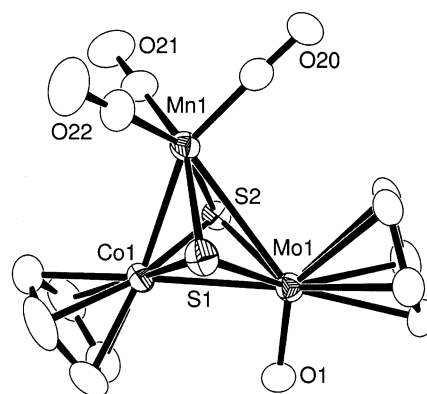


Figure 2. ORTEP diagram of the molecular structure of Cp₂MoMn(CO)₃OC(μ₃-S)₂ (**3**), showing 40% probability thermal ellipsoids.

Table 1. Selected Intramolecular Distances (Å) and Angles (deg) for **2**^a

(a) Distances			
Co(1)–Mn(1)	2.6006(17)	Mn(1)–S(1)	2.2885(16)
Mn(1)–Mo(1)	2.8454(14)	Mo(1)–S(1)	2.4528(14)
Co(1)–S(1)	2.1376(15)	C–O	1.140(10) (av)
(b) Angles			
Co(1)–Mn(1)–Mo(1)	78.66(4)	S(1)–Mn(1)–Mo(1)	55.81(4)
S(1)–Co(1)–S(1a)	86.50(8)	S(1)–Mo(1)–S(1a)	73.33(6)
S(1)–Co(1)–Mn(1)	56.75(5)	S(1)–Mo(1)–Mn(1)	50.52(4)
S(1)–Mn(1)–S(1a)	79.59(8)	Co(1)–S(1)–Mn(1)	71.88(6)
S(1)–Mn(1)–Co(1)	51.37(4)	Co(1)–S(1)–Mo(1)	97.48(5)
S(1a)–Mn(1)–Mo(1)	55.81(4)	Mn(1)S(1)–Mo(1)	73.67(5)

^a Estimated standard deviations in the least significant figure are given in parentheses.

complexes (e.g. Cp₂Mo₂(O)₂[μ-(MeO₂C)C₂(CO₂Me)], Mo–O bond, 1.688(2) and 1.706(2) Å;^{13a} [Cp₂MoWFe₂(O)₂(μ₃-S)₂(CO)₉(CCPh)₂], 1.687(2) Å;^{13b} [Cp₂Mo₂(O)₂(μ-S)₂], 1.705(4) Å^{13c}). Compound **2** is slowly transformed into **3** in air (7% yield in 24 h), but the best yield of **3** (36% in 30 min) was obtained from the reaction of **3** with Me₃NO, which is a better source of oxygen.

The reactions of **1** with Fe₂(CO)₉ and Ru₃(CO)₁₂ respectively yielded the compounds CpMoMnM(CO)₈(μ₃-S)₂ (**4**, M = Fe (71% yield); **5**, M = Ru (17% yield)). A second minor product, CpMoRu₃(CO)₉(μ₃-S)₂(μ-H) (**6**; 4% yield), which contains no manganese, was also obtained from the reaction of **1** with Ru₃(CO)₁₂. The structures of **4** and **5** are similar, and ORTEP diagrams

(11) Boudart, M.; Arrieta, J. S.; Betta, R. D. *J. Am. Chem. Soc.* **1983**, *105*, 6501 and references therein.

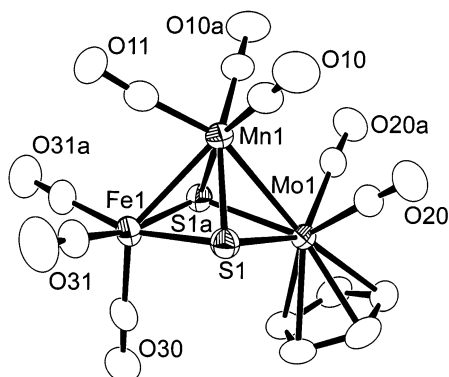
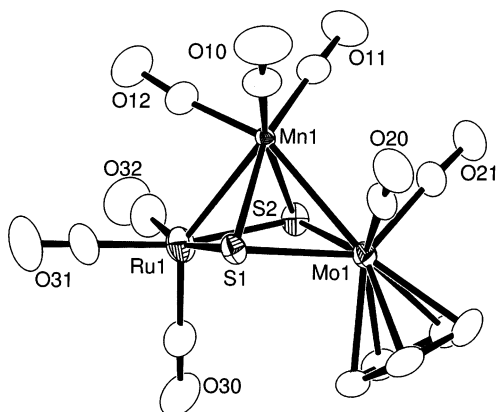
(12) (a) Kullmer, V.; Vahrenkamp, H. *Chem. Ber.* **1977**, *110*, 3810. (b) Challet, S.; Blacque, O.; Gehart, G.; Kubicki, M. M.; Leblanc, J.-C.; Moise, C.; Brunner, H.; Wachter, J. *New J. Chem.* **1997**, *21*, 903.

(13) (a) Stichbury, J. C.; Mays, M. J.; Raithby, P. R.; Rennie, M.-A.; Fullalove, M. R. *J. Chem. Soc., Chem. Commun.* **1995**, 1269. (b) Mathur, P.; Mukhopadhyay, S.; Ahmed, M. O.; Lahiri, G. K.; Chakraborty, S.; Walawalkar, M. G. *Organometallics* **2000**, *19*, 5787. (c) Gorzelli, M.; Nuber, B.; Ziegler, M. L. *J. Organomet. Chem.* **1991**, *412*, 95.

Table 2. Selected Intramolecular Distances (Å) and Angles (deg) for 3^a

(a) Distances			
Co(1)–Mn(1)	2.5536(6)	Mn(1)–S(2)	2.2944(8)
Co(1)–Mo(1)	2.6784(5)	Mo(1)–S(1)	2.3314(7)
Mn(1)–Mo(1)	3.1412(6)	Mo(1)–S(2)	2.3376(7)
Co(1)–S(1)	2.1828(8)	Mo(1)–O	1.706(2)
Co(1)–S(2)	2.1823(8)	C–O	1.143(4) (av)
Mn(1)–S(1)	2.3107(9)		
(b) Angles			
Mn(1)–Co(1)–Mo(1)	73.751(16)	S(1)–Co(1)–Mo(1)	56.21(2)
Co(1)–Mn(1)–Mo(1)	54.947(13)	S(2)–Mn(1)–S(1)	87.71(3)
Co(1)–Mo(1)–Mn(1)	51.302(12)	S(2)–Mn(1)–Co(1)	53.18(2)
S(2)–Co(1)–S(1)	93.93(3)	S(1)–Mn(1)–Co(1)	53.04(2)
S(2)–Co(1)–Mn(1)	57.31(2)	S(1)–Mo(1)–S(2)	86.21(2)
S(1)–Co(1)–Mn(1)	57.76(2)	O(1)–Mo(1)–Co(1)	86.25(7)
S(2)–Co(1)–Mo(1)	56.38(2)	S(1)–Mo(1)–Co(1)	51.09(2)
S(2)–Mn(1)–Mo(1)	47.883(18)	S(1)–Mo(1)–Mn(1)	47.14(2)
S(1)–Mn(1)–Mo(1)	47.70(2)	Co(1)–S(1)–Mn(1)	69.19(2)
O(1)–Mo(1)–S(1)	109.56(8)	Co(1)–S(1)–Mo(1)	72.70(2)
O(1)–Mo(1)–S(2)	108.92(7)	Co(1)–S(2)–Mn(1)	69.50(2)
S(2)–Mo(1)–Co(1)	51.027(19)	Co(1)–S(2)–Mo(1)	72.59(2)
O(1)–Mo(1)–Mn(1)	137.55(7)	Mn(1)–S(2)–Mo(1)	85.39(2)
S(2)–Mo(1)–Mn(1)	46.725(18)		

^a Estimated standard deviations in the least significant figure are given in parentheses.

**Figure 3.** ORTEP diagram of the molecular structure of CpMoMnFe(CO)₈(μ₃-S)₂ (**4**), showing 40% probability thermal ellipsoids.**Figure 4.** ORTEP diagram of the molecular structure of CpMoMnRu(CO)₈(μ₃-S)₂ (**5**), showing 40% probability thermal ellipsoids.

of the molecular structures of these compounds are shown in Figures 3 and 4, respectively. Selected bond distances and angles are listed in Tables 3 and 4, respectively. The structures of **4** and **5** are similar to that of **2**, with the replacement of an M(CO)₃ group for the CpCo group. Each molecule has two triply bridging

Table 3. Selected Intramolecular Bond Distances (Å) and Angles (deg) for 4^a

(a) Distances			
Mo(1)–Mn(1)	2.8330(10)	Mn(1)–S(1)	2.2772(14)
Fe(1)–Mn(1)	2.6414(13)	Fe(1)–S(1)	2.2291(14)
Mo(1)–S(1)	2.4493(12)	C–O	1.127(7) (av)
(b) Angles			
S(1)#1–Mo(1)–S(1)	72.94(6)	S(1)–Mn(1)–Mo(1)	56.01(3)
S(1)–Mo(1)–Mn(1)	50.43(3)	Fe(1)–Mn(1)–Mo(1)	82.31(3)
S(1)–Fe(1)–S(1a)	81.56(7)	Fe(1)–S(1)–Mn(1)	71.76(5)
S(1)–Fe(1)–Mn(1)	54.96(4)	Fe(1)–S(1)–Mo(1)	100.73(5)
S(1)–Mn(1)–S(1a)	79.49(7)	Mn(1)–S(1)–Mo(1)	73.55(4)
S(1)–Mn(1)–Fe(1)	53.27(4)		

^a Estimated standard deviations in the least significant figure are given in parentheses.

Table 4. Selected Intramolecular Bond Distances (Å) and Angles (deg) for 5^a

(a) Distances			
Mo(1)–Mn(1)	2.8101(14)	Mn(1)–S(2)	2.322(3)
Ru(1)–Mn(1)	2.7569(15)	Ru(1)–S(1)	2.322(2)
Mo(1)–S(1)	2.455(2)	Ru(1)–S(2)	2.333(3)
Mo(1)–S(2)	2.464(3)	C–O	1.127(15) (av)
Mn(1)–S(1)	2.323(3)		
(b) Angles			
S(1)–Mo(1)–S(2)	74.52(8)	S(2)–Mn(1)–Ru(1)	53.88(7)
S(2)–Mo(1)–Mn(1)	51.73(7)	S(1)–Mn(1)–Mo(1)	56.17(6)
S(1)–Mo(1)–Mn(1)	51.83(6)	S(2)–Mn(1)–Mo(1)	56.44(7)
S(1)–Ru(1)–S(2)	79.54(9)	Ru(1)–Mn(1)–Mo(1)	83.27(4)
S(1)–Ru(1)–Mn(1)	53.61(6)	Ru(1)–S(1)–Mn(1)	72.81(8)
S(2)–Ru(1)–Mn(1)	53.49(7)	Ru(1)–S(1)–Mo(1)	101.45(9)
S(1)–Mn(1)–S(2)	79.76(10)	Mn(1)–S(1)–Mo(1)	72.00(7)
S(1)–Mn(1)–Ru(1)	53.58(6)	Mn(1)–S(2)–Ru(1)	72.63(8)
Mn(1)–S(2)–Mo(1)	71.84(8)	Ru(1)–S(2)–Mo(1)	100.84(10)

^a Estimated standard deviations in the least significant figure are given in parentheses.

sulfido ligands and eight linear terminal carbonyl ligands. Like **2**, in the solid state compound **4** contains a plane of symmetry that passes through the metal atoms, but this is not the case for compound **5**, which has no crystallographically imposed symmetry in the solid state. The Mn(1)–Mo(1) bond distances for **4** and **5**, 2.8330(10) and 2.8101(14) Å, respectively, are both slightly shorter than the Mn–Mo distance in **2**. The Fe–Mn distance in **4**, 2.6414(13) Å, is longer than the Co–Mn distance in **2**. The Ru(1)–Mn(1) distance in **5**, 2.7569(15) Å, is still longer, as expected for the larger second-row metal ruthenium. The Mo–Fe and Mo–Ru distances in **4** and **5** are both very long, 3.606 and 3.699 Å, and are clearly nonbonding interactions.

An ORTEP diagram of the molecular structure of the minor product **6** is shown in Figure 5. Selected bond distances and angles are listed in Table 5. The molecule contains four metal atoms: one molybdenum and three of ruthenium, and no manganese at all. The four metal atoms are arranged in the form of a butterfly tetrahedron with the molybdenum atom and one ruthenium atom in the “hinge” of the butterfly. There is one triply bridging sulfido ligand on each Ru₂Mo triangular group of metal atoms. Ruthenium atoms Ru(2) and Ru(3) each have three linear terminal carbonyl ligands, but Ru(1) has only two. A hydride ligand was found unexpectedly as a bridging ligand across the Ru(1)–Ru(2) bond, and the Ru(1)–Ru(2) bond distance is significantly longer than the Ru(2)–Ru(3) distance, 2.8418(3) versus 2.8064(3) Å, because of this ligand. The hydride ligand exhibits a very high field shift in the ¹H NMR spectrum, δ –18.52 ppm, as expected for these ligands.

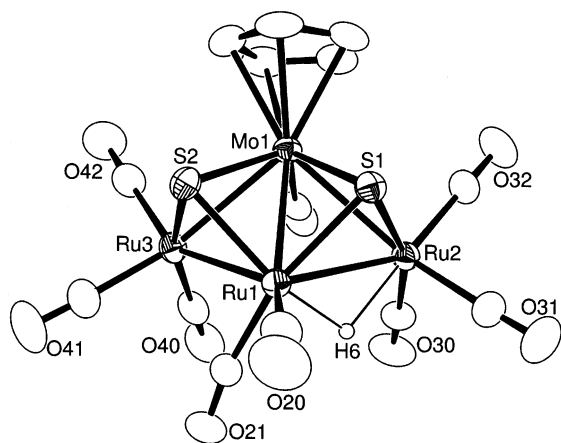


Figure 5. ORTEP diagram of the molecular structure of $\text{CpMoRu}_3(\text{CO})_9(\mu_3\text{-S})_2(\mu\text{-H})$ (**6**), showing 40% probability thermal ellipsoids.

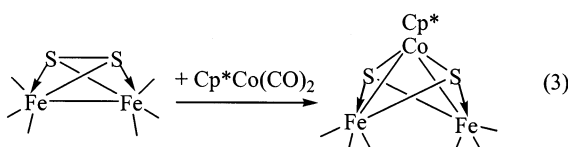
Table 5. Selected Intramolecular Bond Distances (Å) and Angles (deg) for 6^a

(a) Distances			
Ru(1)–S(1)	2.3556(6)	Ru(3)–S(2)	2.3135(6)
Ru(1)–S(2)	2.3416(6)	Ru(3)–Mo(1)	2.8367(3)
Ru(1)–Mo(1)	2.7730(3)	Mo(1)–S(1)	2.3669(6)
Ru(1)–Ru(2)	2.8418(3)	Mo(2)–S(2)	2.3831(6)
Ru(1)–Ru(3)	2.8064(3)	Ru(1)–H(6)	1.75(3)
Ru(2)–S(1)	2.3313(6)	Ru(2)–H(6)	1.86(3)
Ru(2)–Mo(1)	2.9007(3)	C–O	1.134(3) (av)
(b) Angles			
S(2)–Ru(1)–S(1)	86.75(2)	S(1)–Mo(1)–S(2)	85.55(2)
S(2)–Ru(1)–Mo(1)	54.759(15)	S(1)–Mo(1)–Ru(1)	53.852(14)
S(1)–Ru(1)–Mo(1)	54.232(14)	S(2)–Mo(1)–Ru(1)	53.370(15)
S(2)–Ru(1)–Ru(3)	52.466(15)	S(1)–Mo(1)–Ru(3)	113.836(16)
S(1)–Ru(1)–Ru(3)	115.304(16)	S(2)–Mo(1)–Ru(3)	51.730(15)
Mo(1)–Ru(1)–Ru(3)	61.115(7)	Ru(1)–Mo(1)–Ru(3)	60.024(7)
S(2)–Ru(1)–Ru(2)	116.885(16)	S(1)–Mo(1)–Ru(2)	51.322(14)
S(1)–Ru(1)–Ru(2)	52.286(15)	S(2)–Mo(1)–Ru(2)	113.370(16)
Mo(1)–Ru(1)–Ru(2)	62.196(7)	Ru(1)–Mo(1)–Ru(2)	60.066(6)
Ru(3)–Ru(1)–Ru(2)	99.776(8)	Ru(3)–Mo(1)–Ru(2)	97.681(8)
S(1)–Ru(2)–Ru(1)	53.065(15)	Ru(2)–S(1)–Ru(1)	74.649(17)
S(1)–Ru(2)–Mo(1)	52.429(15)	Ru(2)–S(1)–Mo(1)	76.249(17)
Ru(1)–Ru(2)–Mo(1)	57.738(7)	Ru(1)–S(1)–Mo(1)	71.916(17)
S(2)–Ru(3)–Ru(1)	53.383(15)	Ru(3)–S(2)–Ru(1)	74.151(18)
S(2)–Ru(3)–Mo(1)	53.973(16)	Ru(3)–S(2)–Mo(1)	74.298(17)
Ru(1)–Ru(3)–Mo(1)	58.861(7)	Ru(1)–S(2)–Mo(1)	71.871(17)

^a Estimated standard deviations in the least significant figure are given in parentheses.

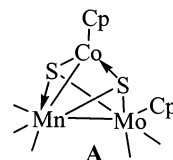
Discussion

A summary of the results of this study is shown in Scheme 1. The reaction of **1** with $\text{CpCo}(\text{CO})_2$ yields compound **2** by the insertion of a cyclopentadienylcobalt grouping into the S–S bond of **1** with the formation of one metal–metal bond between the manganese atom and the cobalt atom. In contrast, the reaction of $\text{Cp}^*\text{Co}(\text{CO})_2$ with $\text{Fe}_2(\text{CO})_6(\mu\text{-S}_2)$ yielded the product $\text{Cp}^*\text{CoFe}_2(\text{CO})_6(\mu_3\text{-S})_2$, in which two Co–Fe bonds were formed and the Fe–Fe bond was cleaved (eq 3).^{3c} $\text{CpCo}(\text{CO})_2$ is

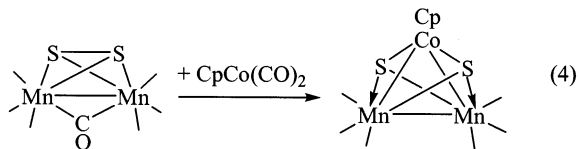


known to lose CO readily to form Co–S bonds with other compounds as well.^{3c,8b,14} Although only one metal–metal bond is formed in the formation of **2**, all metal

atoms still have 18-electron configurations because there is a different distribution of the electron donations from the sulfur atoms to the metal atoms (see structure **A**). The reaction of $\text{Mn}_2(\text{CO})_7(\mu\text{-S}_2)$ with $\text{CpCo}(\text{CO})_2$ also

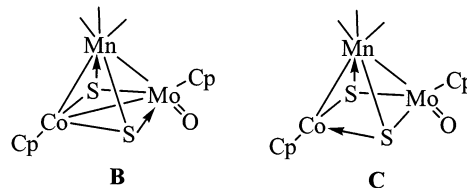


proceeded by insertion of a CpCo group into the S–S bond with formation of two metal–metal bonds to the cobalt atom, eq 4.^{8b} Unlike the reaction with the iron



compound (eq 3), the manganese–manganese bond was not cleaved. This is because the manganese reagent loses one of its CO ligands in the course of the cobalt addition and the iron compound did not lose any of its CO ligands.

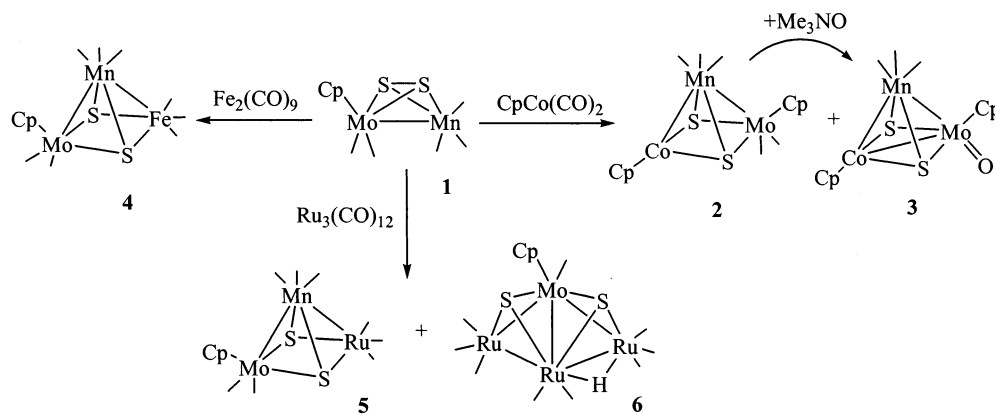
The side product **3** was also formed in the reaction of **1** with $\text{CpCo}(\text{CO})_2$. It contains two fewer CO ligands than **2**, and it has an oxo ligand on the molybdenum atom. The product may have been formed from **2** by reaction with adventitious oxygen either in the original reaction solution or during the separation by TLC that was done in air, and we showed independently that **3** can be obtained from **2** by reaction with air. However, compound **3** can be prepared in a much better yield by reaction of **2** with Me_3NO , which is a more reactive source of oxygen. Compound **3** contains both a Co–Mn bond and a Co–Mo bond, and all metal atoms can have 18-electron configurations, as shown in structure **B**.



However, one can also imagine the structure **C** having different distributions of electron donation from the sulfido ligands and no Co–Mo bond. For structure **C** the Mo atom formally has only 16 valence electrons. We think that the short Co–Mo bond distance in **2** indicates that the structure **B** is the more appropriate one.

The reactions of **1** with $\text{Fe}_2(\text{CO})_9$ and $\text{Ru}_3(\text{CO})_{12}$ yielded the trimetallic complexes **4** and **5** analogous to **2**, which contain $\text{M}(\text{CO})_3$ groups ($\text{M} = \text{Fe}, \text{Ru}$, respectively) in place of the CpCo group in **2**. These reactions probably proceed by insertion of a $\text{M}(\text{CO})_x$ fragment into the S–S bond of **1**. The yield of **5** is significantly lower than that of **4**, probably because $\text{Ru}_3(\text{CO})_{12}$ does not provide $\text{M}(\text{CO})_x$ fragments as readily as $\text{Fe}_2(\text{CO})_9$. The unexpected product **6** was also obtained from the

Scheme 1



reaction of **1** with $\text{Ru}_3(\text{CO})_{12}$. Compound **6** was evidently formed by the addition of the entire triruthenium group to **1**. Surprisingly, the $\text{Mn}(\text{CO})_3$ group in **1** was displaced and a hydride ligand was added. The source of the hydride ligand was not identified in this study. We can only speculate that it probably came from adventitious water or some other protic compound in the reaction solvents.

Experimental Section

General Data. All reactions were performed under a nitrogen atmosphere using Schlenk techniques. Reagent grade solvents were dried by the standard procedures and were freshly distilled prior to use. Infrared spectra were recorded on a Thermo-Nicolet Avatar FTIR spectrophotometer. ^1H NMR spectra were recorded on a Varian Inova 300 spectrometer operating at 300 MHz. Mass spectra were recorded on a VG70SQ mass spectrometer. Elemental analyses were performed by Desert Analytics (Tucson, AZ). $\text{CpCo}(\text{CO})_2$, $\text{Fe}_2(\text{CO})_9$, and $\text{Ru}_3(\text{CO})_{12}$ were purchased from Strem and were used without further purification. Product separations were performed by TLC in air on Analtech 0.25 and 0.5 mm silica gel 60 Å F_{254} glass plates. $\text{CpMoMn}(\text{CO})_5(\mu\text{-S}_2)$ was prepared according to our recently published procedure.⁹

Reaction of 1 with $\text{CpCo}(\text{CO})_2$. A solution of $\text{CpMoMn}(\text{CO})_5(\mu\text{-S}_2)$ (20.0 mg, 0.0476 mmol) in THF (20 mL) was allowed to react with 30 μL of $\text{CpCo}(\text{CO})_2$. The resulting solution was stirred at room temperature for 12 h. After the mixture was stirred, the volatiles were removed in vacuo and the residue was separated by TLC on silica gel using a hexane/ CH_2Cl_2 (2/1 v/v) solvent mixture. A 5.0 mg amount of unreacted **1**, 10.3 mg of $\text{Cp}_2\text{MoCoMn}(\text{CO})_5(\mu_3\text{-S})_2$ (**2**; 40% yield) and 5.0 mg of $\text{Cp}_2\text{MoCoMn}(\text{CO})_3\text{O}(\mu_3\text{-S})_2$ (**3**; 21% yield) were obtained in order of elution. Spectral data for **2**: IR (cm^{-1} in CH_2Cl_2) ν_{CO} 2021 (s), 1969 (m), 1959 (m), 1903 (w); ^1H NMR (δ in CDCl_3) 5.31 (s, 5H), 5.23 (s, 5H); MS (DEP) m/z 518 ($\text{M}^+ - \text{CO}$), 462 ($\text{M}^+ - 3\text{CO}$), 434 ($\text{M}^+ - 4\text{CO}$), 406 ($\text{M}^+ - 5\text{CO}$). Spectral data for **3**: IR (cm^{-1} in KBr disk) ν_{CO} 1990 (s), 1928 (vs), 1897 (vs), 1867 (w), $\nu(\text{Mo}=\text{O})$ 895 (m); ^1H NMR (δ in CDCl_3) 5.54 (s, 5H), 4.78 (s, 5H); MS (FAB) m/z 506 ($\text{M} + 2$), 422 ($\text{M} - 3\text{CO}$, 100). Anal. Calcd for $\text{C}_{13}\text{H}_{10}\text{CoMnMoO}_4\text{S}_2$: C, 30.97; H, 2.00. Found: C, 31.04; H, 2.03.

Reaction of 2 with Air. A THF (10 mL) solution of **2** (12 mg, 0.022 mmol) was stirred at room temperature in air for 24 h. The solvent was removed, and the residue was separated by TLC on silica gel by using a hexane/ CH_2Cl_2 (2/1 v/v) solvent mixture. A 0.8 mg amount of **2** and 0.8 mg of **3** (7% yield) were obtained in order of elution.

Reaction of 2 with $\text{Me}_3\text{NO}\cdot 2\text{H}_2\text{O}$. A 3.6 mg amount of **2** (0.0066 mmol) was dissolved in 10 mL of THF containing 3.0 mg (0.027 mmol) of $\text{Me}_3\text{NO}\cdot 2\text{H}_2\text{O}$. After the mixture was

stirred at room temperature for 30 min, the solvent was removed and the mixture was separated by TLC to give 1.2 mg of **3** (36% yield).

Reaction of 1 with $\text{Fe}_2(\text{CO})_9$. A 20.0 mg (0.0476 mmol) amount of **1** was dissolved in 30 mL of distilled THF in a 100 mL three-neck round-bottom flask equipped with a stir bar, gas inlet, and gas outlet. To this solution was added 26.0 mg (0.071 mmol) of $\text{Fe}_2(\text{CO})_9$. The solution was stirred at room temperature for 24 h. The solvent was then removed in vacuo, and the residue was separated by TLC on silica gel by using a 3/1 hexane/ CH_2Cl_2 solvent mixture to yield 19 mg (71%) of $\text{CpMoMnFe}(\text{CO})_8(\mu_3\text{-S})_2$ (**4**). Spectral data for **4**: IR (cm^{-1} in hexane) ν_{CO} 2072 (m), 2032 (s), 2015 (m), 1990 (m), 1948 (w), 1925 (m); ^1H NMR (δ in CDCl_3) 5.62 (s, 5H). Anal. Calcd for $\text{C}_{13}\text{H}_5\text{FeMnMoO}_3\text{S}_2$: C, 27.88; H, 0.90. Found: C, 27.44; H, 0.85.

Reaction of 1 with $\text{Ru}_3(\text{CO})_{12}$. To a solution of **1** (25 mg, 0.0595 mmol) in THF (30 mL) was added 38 mg (0.0594 mmol) of $\text{Ru}_3(\text{CO})_{12}$. The solution was refluxed for 5 h. Then the solvent was removed in vacuo, and the residue was separated by TLC on silica gel using a 3/1 hexane/ CH_2Cl_2 solvent mixture to yield 1.7 mg (4%) of $\text{CpMoRu}_3(\text{CO})_9(\mu_3\text{-S})_2(\mu\text{-H})$ (**6**) and 6.1 mg (17%) of $\text{CpMoMnRu}(\text{CO})_8(\mu_3\text{-S})_2$ (**5**) in order of elution. Spectral data for **5**: IR (cm^{-1} in hexane) ν_{CO} 2086 (m), 2033 (vs), 2026 (s), 2019 (m), 1997 (m), 1979 (m), 1943 (w), 1917 (w); ^1H NMR (δ in CDCl_3) 5.603 (s, 5H). Anal. Calcd for $\text{C}_{13}\text{-H}_5\text{MoMnRuO}_3\text{S}_2$: C, 25.80; H, 0.83. Found: C, 25.90; H, 0.90. Spectral data for **6**: IR (cm^{-1} in CH_2Cl_2) ν_{CO} 2091 (m), 2069 (vs), 2025 (s), 2010 (s); ^1H NMR (δ in CDCl_3) 5.61 (s, 5H), -18.52 (s, 1H). MS (EI) m/z 781.8 - $n(28)$, $n = 1-9$ ($\text{M}^+ - n(\text{CO})$).

Crystallographic Analysis. Dark red crystals of **2** and **4-6** were grown by slow evaporation of solvent from a solution in a hexane/methylene chloride solvent mixture at -20°C . Dark red single crystals of **3** suitable for diffraction analysis were grown by slow evaporation of solvent from a hexane solution at 4°C . The data crystals of all compounds were mounted by gluing onto the end of a thin glass fiber. X-ray intensity data were measured by using a Bruker SMART APEX CCD-based diffractometer by using $\text{Mo K}\alpha$ radiation ($\lambda = 0.71073 \text{ \AA}$). All unit cells were initially determined on the basis of reflections selected from a set of three scans measured in orthogonal wedges of reciprocal space. The raw data frames were integrated with the SAINT+ program using a narrow-frame integration algorithm.¹⁵ Corrections for the Lorentz and polarization effects were also applied by using the program SAINT. An empirical absorption correction based on the multiple measurement of equivalent reflections was applied for each analysis by using the program SADABS. Crystal data, data collection parameters, and results of the

(15) SAINT+, version 6.02a; Bruker Analytical X-ray Systems, Inc., Madison, WI, 1998.

Table 6. Crystallographic Data for Compounds 2–6

	2	3	4	5	6
empirical formula	C ₁₆ H ₁₂ Cl ₂ CoMnMoO ₅ S ₂	C ₁₃ H ₁₀ CoMnMoO ₄ S ₂	C ₁₃ H ₅ FeMnMoO ₈ S ₂	C ₁₃ H ₅ MnMoRuO ₈ S ₂	C ₁₄ H ₆ MoO ₉ Ru ₃ S ₂
fw	629.09	504.14	560.02	605.24	781.46
cryst syst	monoclinic	monoclinic	monoclinic	monoclinic	orthorhombic
space group	<i>C2/m</i>	<i>P2₁/n</i>	<i>P2₁/m</i>	<i>P2₁/c</i>	<i>Pbca</i>
<i>a</i> (Å)	15.1536(11)	8.6984(9)	8.7632(7)	9.1997(8)	13.1515(7)
<i>b</i> (Å)	9.7595(7)	21.182(2)	11.8155(9)	17.2187(15)	16.8260(9)
<i>c</i> (Å)	14.7202(12)	9.4883(9)	9.0910(7)	12.2118(11)	18.6984(10)
β (deg)	99.350(5)	113.136(2)	107.133(2)	109.340(2)	90
<i>V</i> (Å ³)	2148.1(3)	1607.6(3)	899.52(12)	1825.3(3)	4137.7(4)
<i>Z</i>	4	4	2	4	8
temp (K)	294(2)	296(2)	293(2)	296(2)	294(2)
ρ_{calcd} (g/cm ³)	1.945	2.083	2.068	2.202	2.509
μ (Mo K α) (mm ⁻¹)	2.38	2.83	2.44	2.44	2.985
no. of observns (<i>I</i> > 2 σ (<i>I</i>))	2304	3471	1977	3149	4584
no. of params	142	199	130	235	266
goodness of fit ^a	1.052	1.087	1.093	1.042	1.051
max shift in final cycle	0.001	0.000	0.000	0.001	0.002
residuals: R1; wR2 ^b	0.0590; 0.1944	0.0306; 0.0696	0.0486; 0.1152	0.0703; 0.2149	0.0193; 0.0461
abs cor, max/min	SADABS, 1.000/0.802	SADABS, 1.000/0.883	SADABS, 1.000/0.797	SADABS, 1.000/0.679	SADABS, 1.0000/0.8395
largest peak in diff map (e/Å ³)	1.670	0.520	1.297	2.614	0.562

$$^a \text{GOF} = [\sum_{hkl}(w(|F_o| - |F_c|))^2 / (n_{\text{data}} - n_{\text{vari}})]^{1/2}. \quad ^b \text{R1} = \sum(|F_o| - |F_c|) / \sum |F_o|. \quad \text{wR2} = \{\sum [w(F_o^2 - F_c^2)^2 / \sum w(F_o^2)^2]\}^{1/2}; \quad w = 1/\sigma^2(F_o^2).$$

analyses for compounds 2–6 are listed in Table 6. All structures were solved by a combination direct methods and difference Fourier syntheses. All non-hydrogen atoms were refined with anisotropic thermal parameters. The positions of the hydrogen atoms were calculated by assuming idealized geometries and were refined by using the riding model. Refinements were carried out on F^2 by the method of full-matrix least squares by using the SHELXTL program library with neutral atom scattering factors.¹⁶ Compound 2 crystallized in the monoclinic crystal system. The systematic absences in the data were consistent with the space groups *C2/m*, *Cm*, and *C2*. The centric space group *C2/m* was tested first and confirmed by the successful solution and refinement of the structure. In the solid state the molecule possesses a crystallographically imposed reflection symmetry. One equivalent of CH₂Cl₂ from the solvent of crystallization was found cocrystallized with the complex. This molecule of CH₂Cl₂ was successfully refined with anisotropic thermal parameters. Compound 3 crystallized in the monoclinic crystal system. The space group *P2₁/n* was uniquely identified on the basis of the systematic absences observed in the data. All non-hydrogen atoms were refined with anisotropic displacement parameters.

Compound 4 crystallized in the monoclinic crystal system. The systematic absences in the data were consistent with either of the space groups *P2₁/m* and *P2₁*. The centric space group *P2₁/m* was tested first and confirmed by the successful solution and refinement of the structure. In the solid state the molecule possesses a crystallographically imposed reflection symmetry. Compounds 5 and 6 crystallized in the monoclinic and orthorhombic crystal systems, respectively. The space groups *P2₁/c* and *Pbca* were uniquely identified on the basis of the systematic absences observed in the data. All non-hydrogen atoms were refined with anisotropic displacement parameters.

Acknowledgment. This research was supported by a grant from the National Science Foundation, Grant No. CHE-9909017. We thank Dr. Burjor Captain and Dr. Qian-feng Zhang for assistance with the structural analyses.

Supporting Information Available: Tables giving X-ray crystallographic data for the structural analyses of 2–6. This material is available free of charge via the Internet at <http://pubs.acs.org>.

OM030141K

(16) Sheldrick, G. M. SHELXTL, version 5.1; Bruker Analytical X-ray Systems, Inc., Madison, WI, 1997.